



Photon and jet probes of small collision systems with ATLAS

Martin Spousta
for ATLAS collaboration

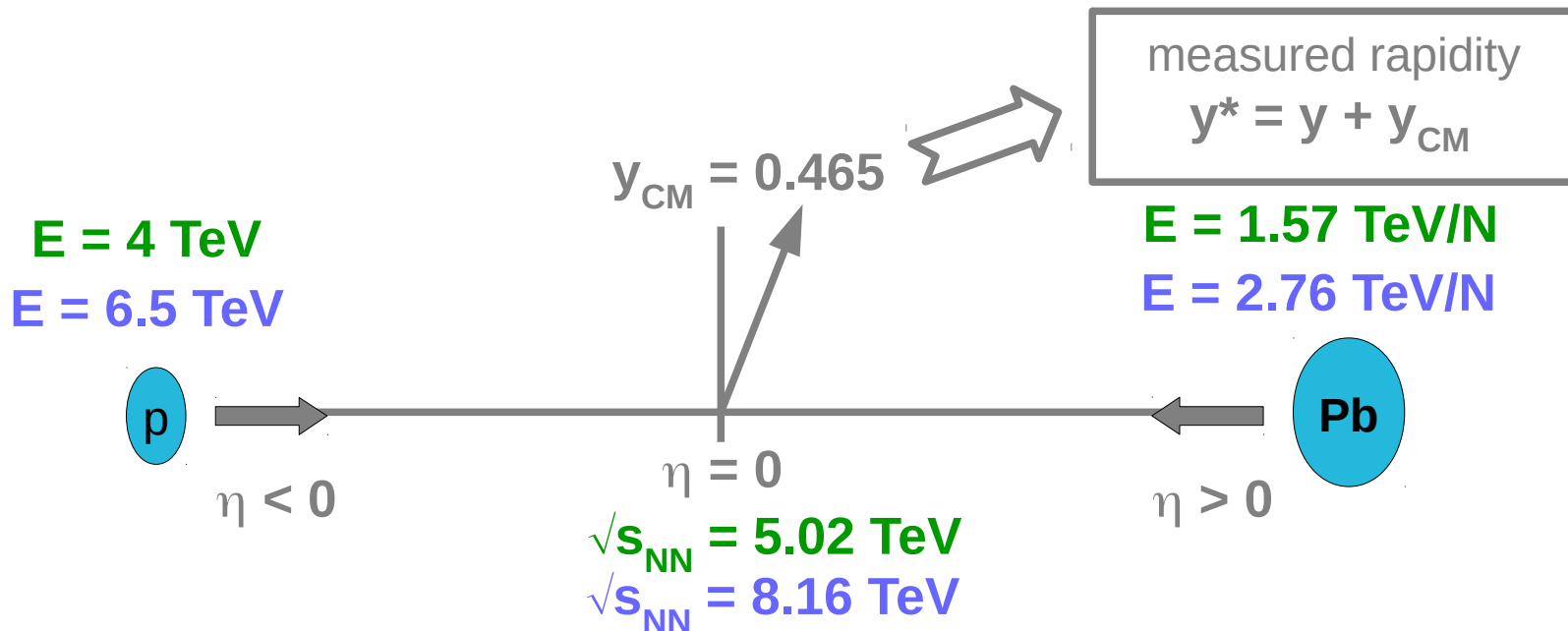
Charles University,
Prague

9th International Conference on Hard & Electromagnetic Probes
of High-Energy Nuclear Collisions, Aix-Les-Bains, France

- Original motivation for p+Pb collisions:
 - to calibrate Pb+Pb measurements,
 - to understand initial state effects,
 - to study nuclear PDFs, ...
 - **ATLAS results** in p+Pb collisions:
 - Charged particle spectra, multiplicities, R_{pPb}
 - Ridge and flow, HBT correlations
 - Jet production and fragmentation
 - W and Z boson production, gamma production
 - Quarkonia and heavy flavor production
- ... quite a lot of unexpected seen! p+Pb is a non-trivial reference

- Original motivation for p+Pb collisions:
 - to calibrate Pb+Pb measurements,
 - to understand initial state effects,
 - to study nuclear PDFs, ...
- **ATLAS results** in p+Pb collisions:
 - Charged particle spectra, multiplicities, R_{pPb}
 - [ATLAS-CONF-2018-050](#) relations
 - **Jet production** and fragmentation [ATLAS-CONF-2017-072](#)
 - W and Z boson production, **gamma production**
 - Quarkonia and heavy flavor production
 - [Talk by Sebastia Tapia](#) ([Talk by Mirta Dumancic](#)) non-trivial reference
- Here only selected new results on jets and photons.

System	Year	$\sqrt{s_{NN}}$ [TeV]	L_{int}
$p+Pb$	2012	5.02	$1 \mu b^{-1}$
$p+Pb$	2013	5.02	29 nb^{-1}
$p+Pb$	2016	5.02	0.5 nb^{-1}
$p+Pb$	2016	8.16	180 nb^{-1}



Prompt photons

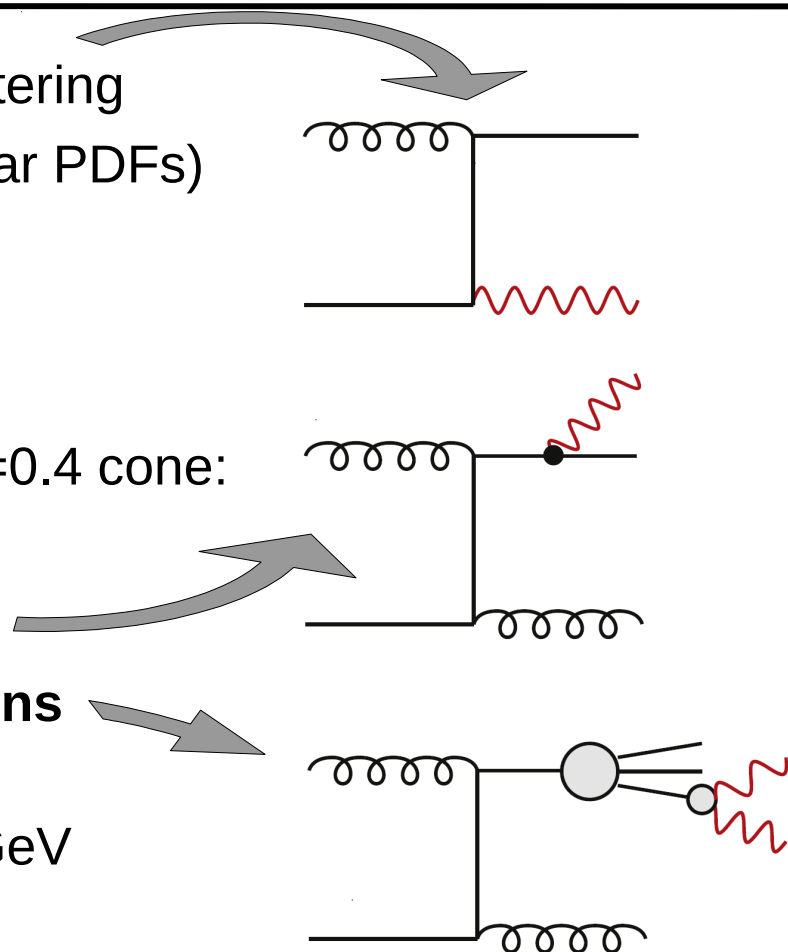


- **Prompt photons** originate in initial hard scattering
 - Sensitive to initial state densities (nuclear PDFs) and potential initial state energy loss.
 - Insensitive to final state modification.

- **Isolation** requirement:

- Reject photons w/ excess E_T within $\Delta R=0.4$ cone:
 $E_T > E_{T,iso} = 4.8 + 4.2 \times 10^{-3} E_{T\gamma}$ [GeV]
- Suppresses of **fragmentation** photons
- Suppresses photons from **vector mesons** decays

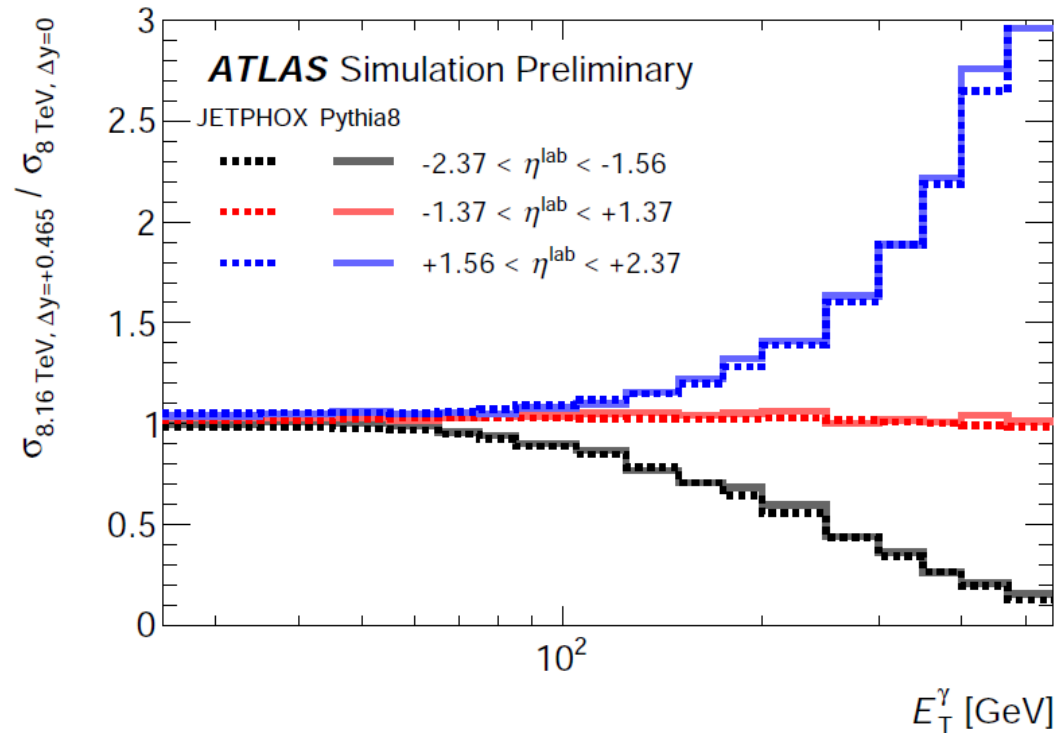
- Measurement performed for $25 < E_{T\gamma} < 500$ GeV in three bins of η^* between -2.83 and 1.91.
- First LHC measurement of isolated prompt (or direct) photons in p+Pb collisions.

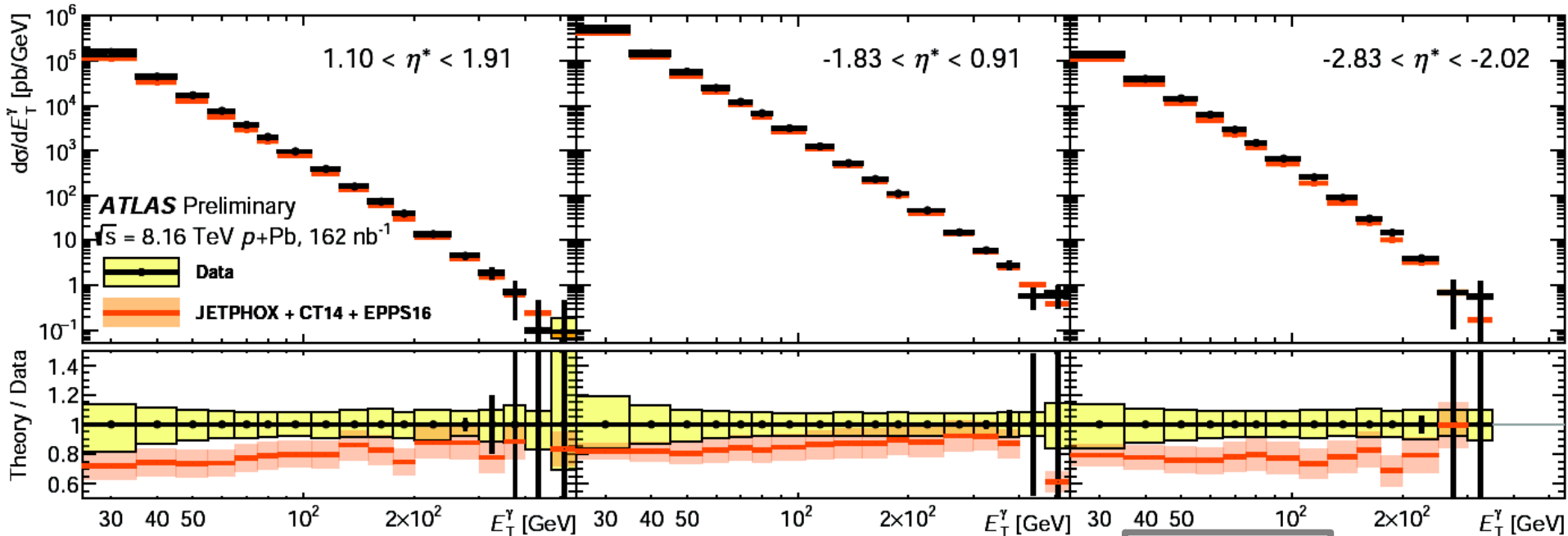


- No pp data exists at 8.16 TeV => **extrapolation**
- Photon cross-section calculated in **JETPHOX** for 8 TeV and 8.16 TeV
- Correction factors:

$$\sigma_{8.16 \text{ TeV}, \Delta y=+0.465} / \sigma_{8 \text{ TeV}, \Delta y=0}$$

... applied on **data from 8 TeV pp collisions** (JHEP 08 (2016) 005).



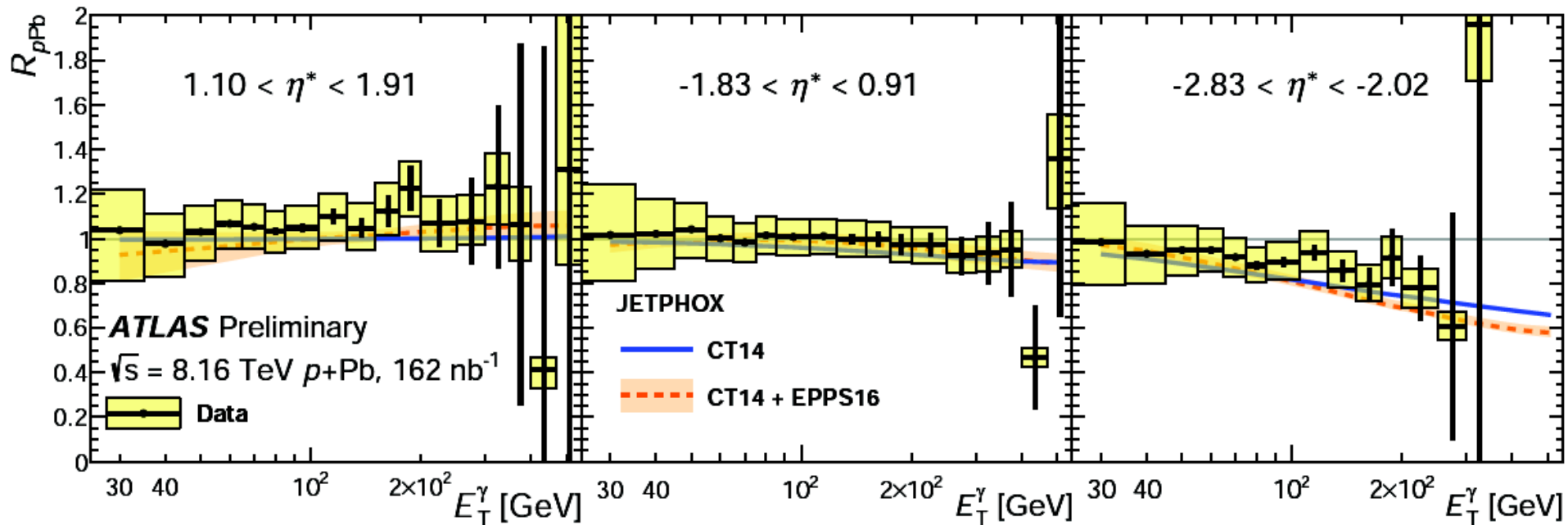


$$d\sigma / dE_T^\gamma = \frac{1}{L_{\text{int}}} \frac{1}{\Delta E_T^\gamma} \frac{N_{\text{sig}} P_{\text{sig}}}{\epsilon^{\text{sel}} \epsilon^{\text{trig}}} C$$

Purity (points to P_{sig})
 bin-by-bin (points to C)
 Efficiencies (points to $\epsilon^{\text{sel}} \epsilon^{\text{trig}}$)

Cross-section in pp compared to JETPHOX – similar level of **disagreement** as in previous pp photon measurement ([JHEP 08 \(2016\) 005](#), [PLB 770 \(2017\) 473](#)).

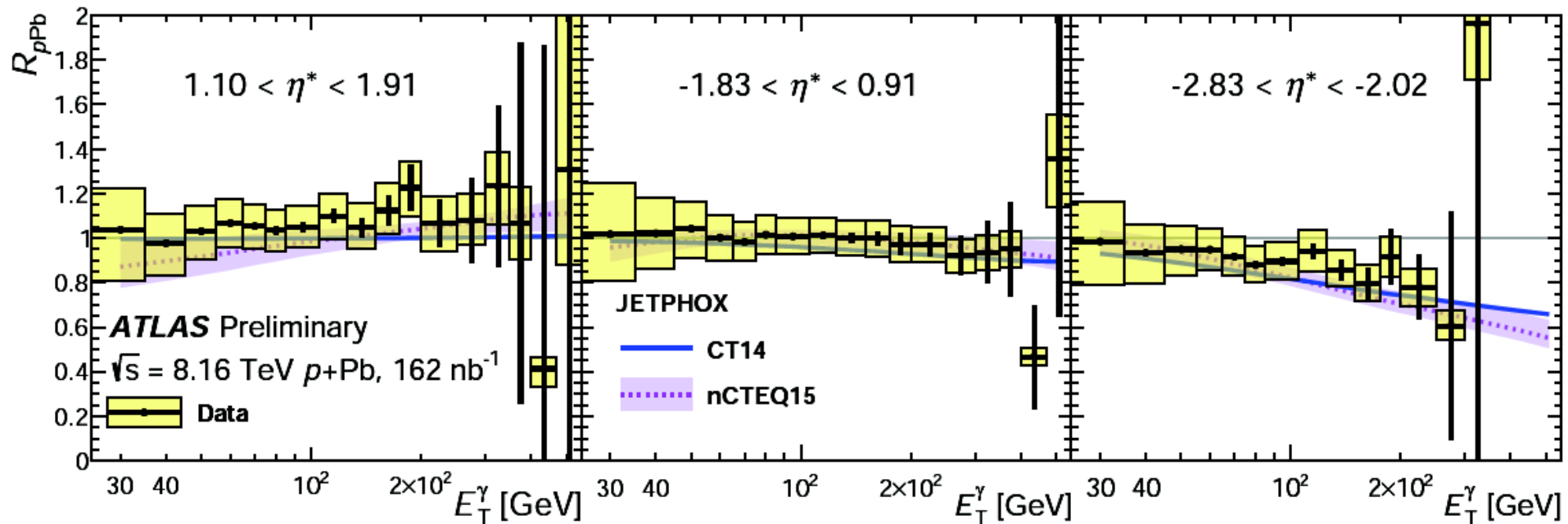
$$R_{pPb} = (d\sigma^{P+Pb \rightarrow \gamma+X} / dE_T^\gamma) / (A \cdot d\sigma^{PP \rightarrow \gamma+X} / dE_T^\gamma)$$



- Consistent with unity except for backward (Pb-going) direction: consistent with **expected isospin effects**.
- Data compared to two nPDF sets: **CT14+EPPS16**, nCTEQ15 – **no ability to distinguish**.

Thanks to I. Helenius and H. Paukunen for nPDF calculations

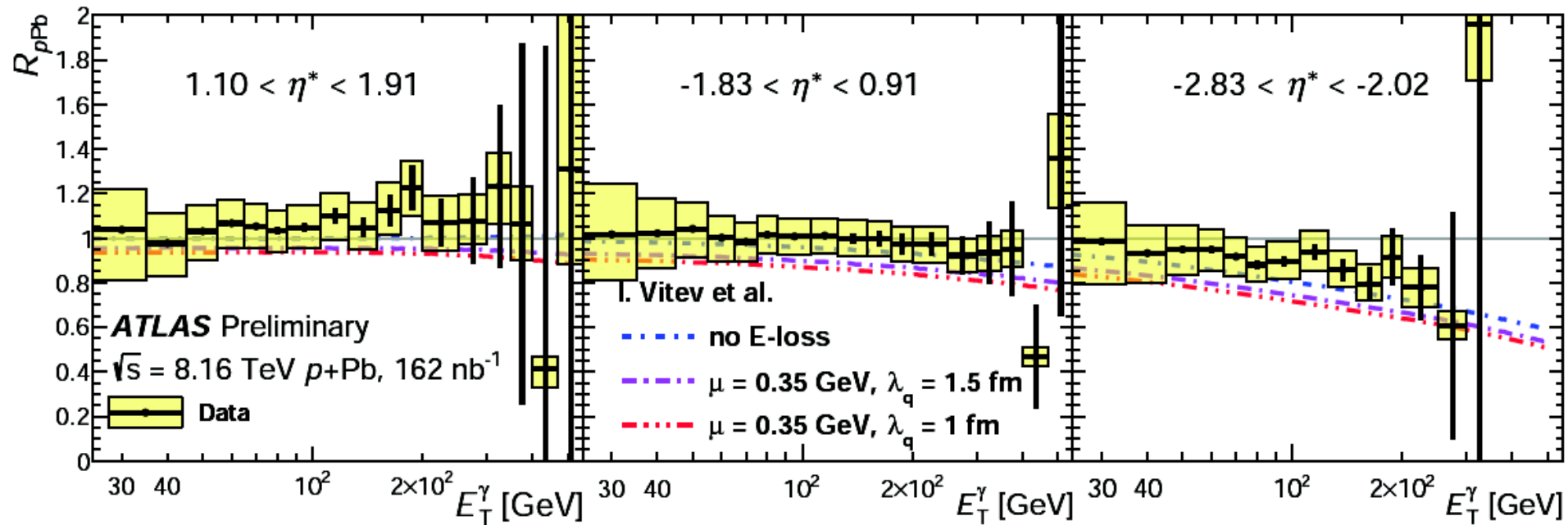
$$R_{pPb} = (d\sigma^{P+Pb \rightarrow \gamma+X} / dE_T^\gamma) / (A \cdot d\sigma^{PP \rightarrow \gamma+X} / dE_T^\gamma)$$



- Consistent with unity except for backward (Pb-going) direction: consistent with **expected isospin effects**.
- Data compared to two nPDF sets: CT14+EPPS16, **nCTEQ15 – no ability to distinguish**.

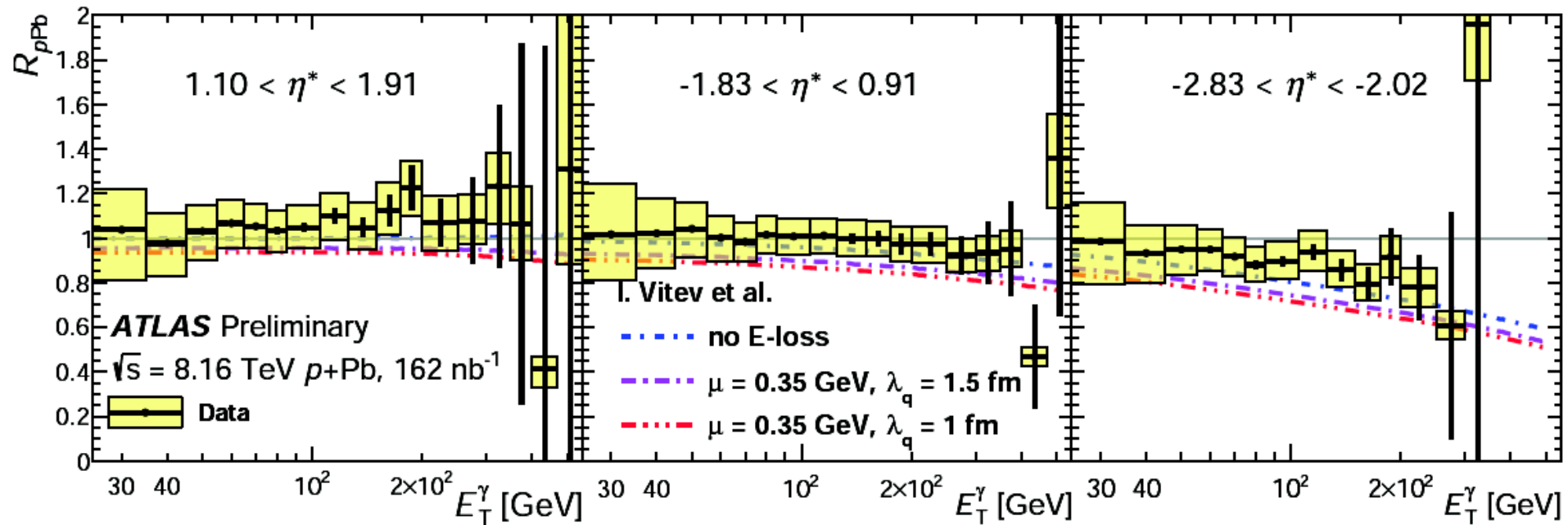
Thanks to I. Helenius and H. Paukunen for nPDF calculations

$$R_{pPb} = (d\sigma^{P+Pb \rightarrow \gamma+X} / dE_T^\gamma) / (A \cdot d\sigma^{PP \rightarrow \gamma+X} / dE_T^\gamma)$$



- Consistent with unity except for backward (Pb-going) direction = consistent with **expected isospin effects**.
- Data compared to two energy loss scenarios: **no sign of energy loss**.

$$R_{pPb} = (d\sigma^{P+Pb \rightarrow \gamma+X} / dE_T^\gamma) / (A \cdot d\sigma^{PP \rightarrow \gamma+X} / dE_T^\gamma)$$

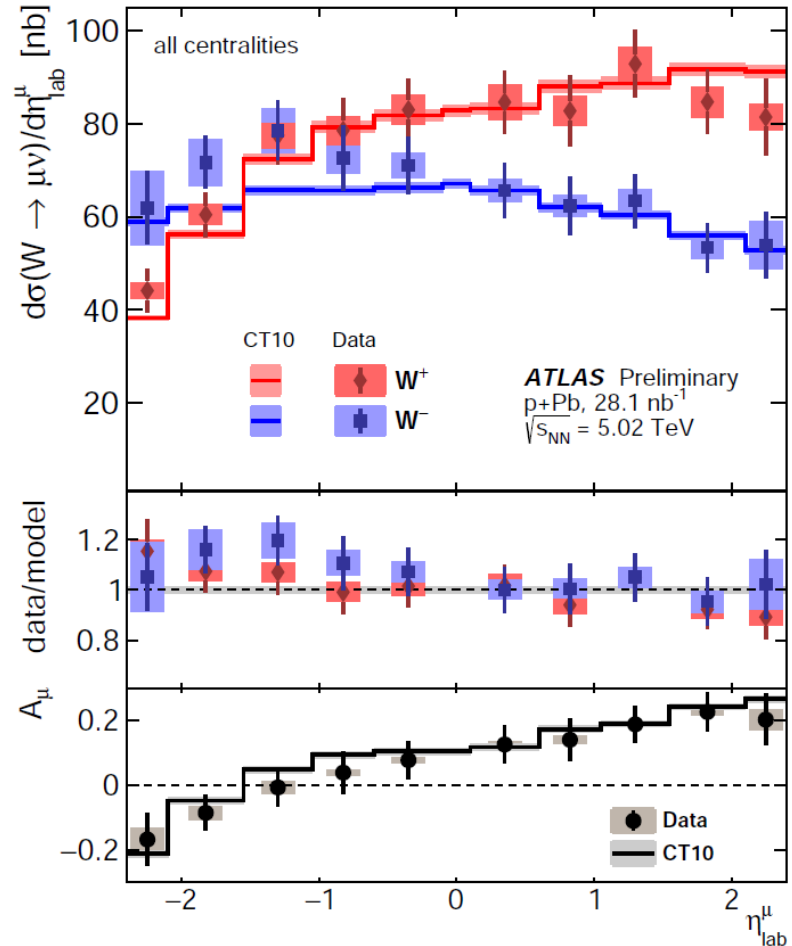
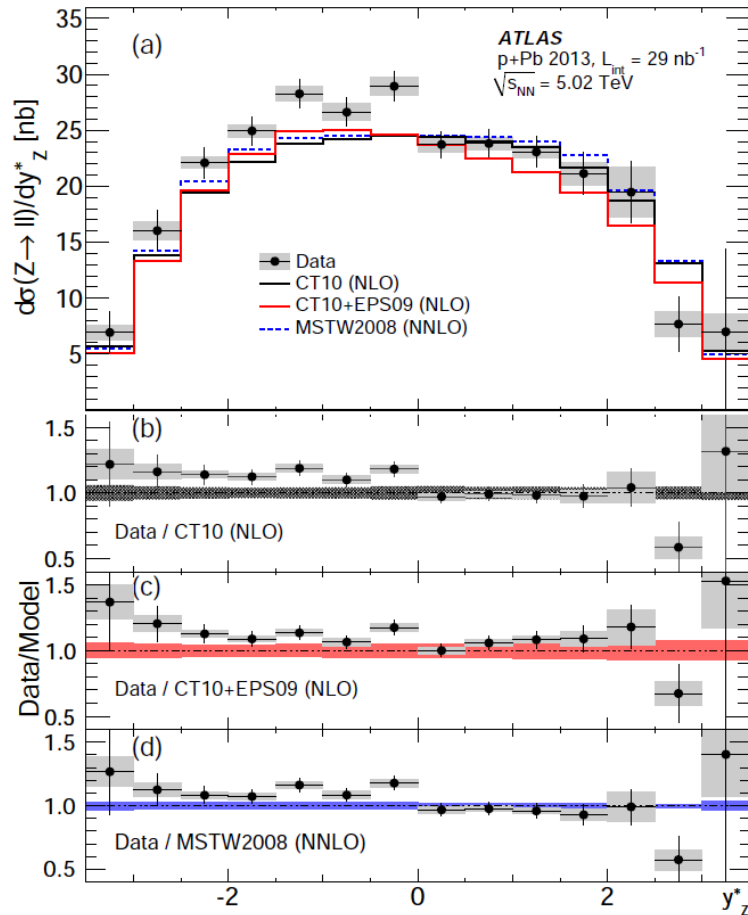


Outlook:

- Final results coming up soon with **significant reduction** of systematic uncertainties.
- **Forward-to-backward** ratio to be added.

Phys. Rev. C 92, 044915 (2015)

ATLAS-CONF-2015-056



... no ability to distinguish nPDF effects, data consistent with NLO pQCD

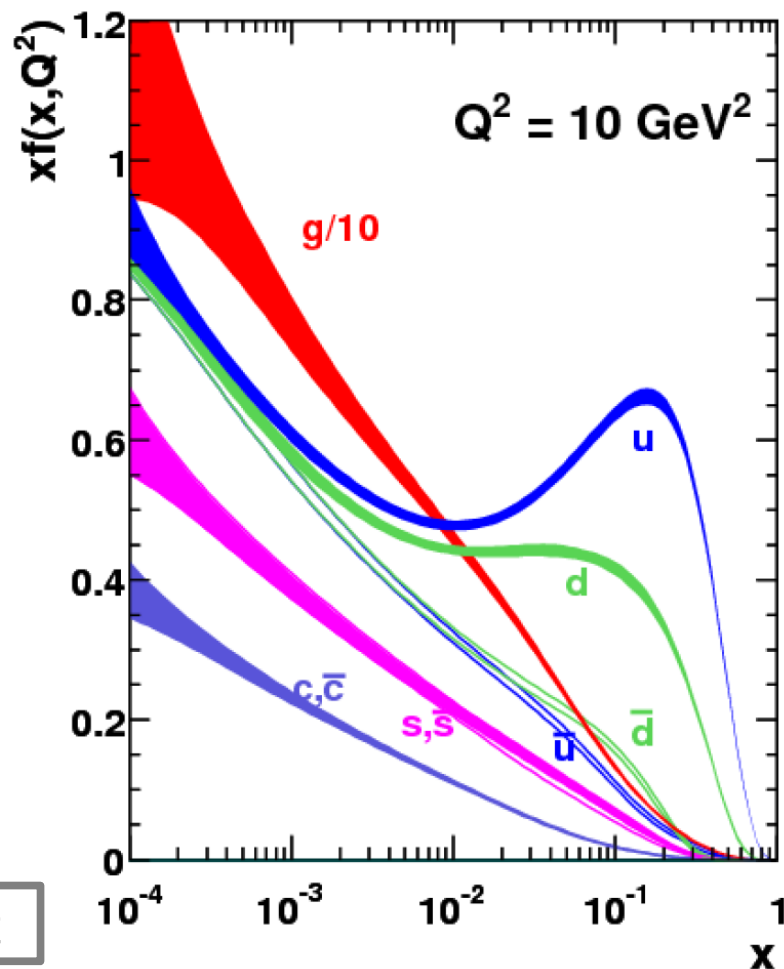
Dijet $\Delta\phi$ correlations

- **Steep rise** of gluon PDFs at low- x versus unitarity.
- **Saturation** can bring expected change of trend at low- x .
- Saturation studied **before**, e.g. using high- p_T charged particles.
- **Dijet $\Delta\phi$ correlations** sensitive to saturation effects.

$$\Delta\phi = |\phi_1 - \phi_2|$$

Leading jet

Sub-leading jet



Correlation function

$$C_{12} = \frac{1}{N_1} \frac{dN_{1,2}}{d\Delta\phi}$$



$$W_{12} = \text{RMS}(C_{12})$$



$$\rho_W^{pPb} = \frac{W_{12}^{p+Pb}}{W_{12}^{pp}}$$

Dijet conditional yield

$$I_{12} = \frac{1}{N_1} \frac{dN_{1,2}}{dy_1^* dy_2^* dp_{T,1} dp_{T,2}}$$



$$\rho_I^{pPb} = \frac{I_{12}^{p+Pb}}{I_{12}^{pp}}$$

Correlation function

$$C_{12} = \frac{1}{N_1} \frac{dN_{1,2}}{d\Delta\phi}$$

Dijet conditional yield

$$I_{12} = \frac{1}{N_1} \frac{dN_{1,2}}{dy_1^* dy_2^* dp_{T,1} dp_{T,2}}$$

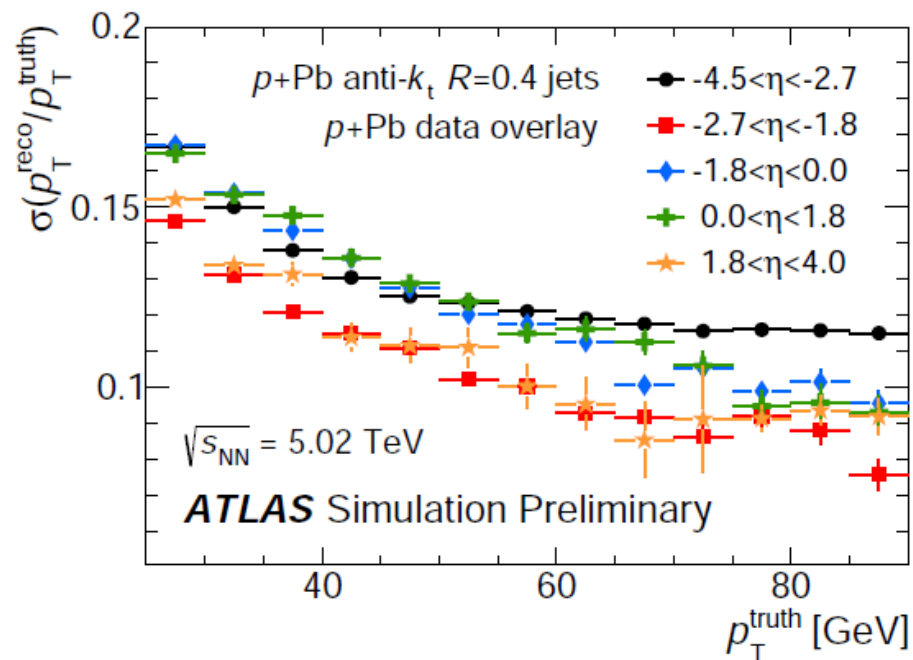
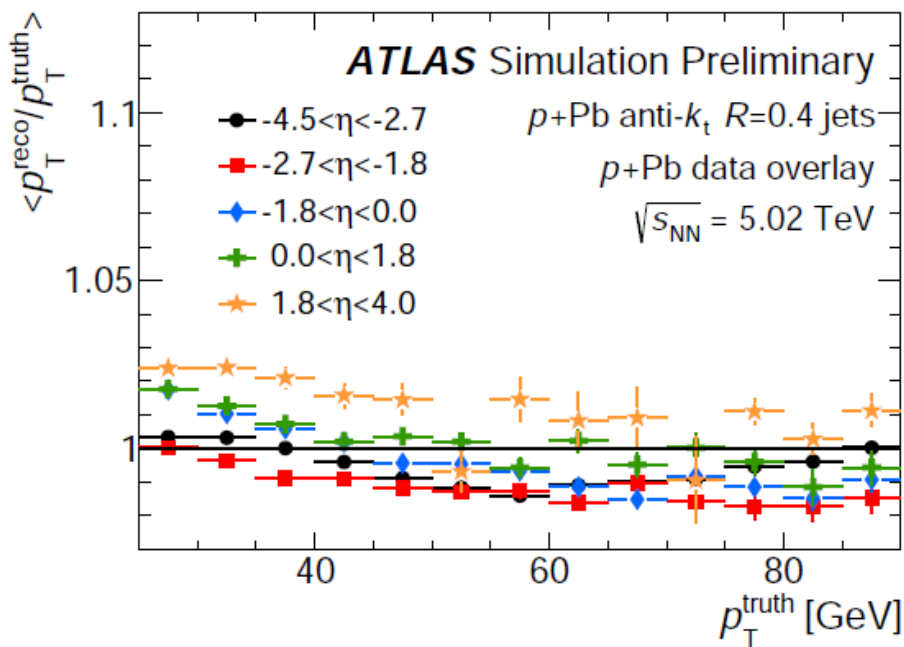
$$W_{12} = \text{RMS}(C_{12})$$

$$C_{12}(\Delta\Phi) = \int_{-\infty}^{\infty} d\delta \frac{e^{-\delta^2/2\sigma^2}}{\sqrt{8\pi\sigma^2\tau^2}} e^{-|\Delta\Phi-\delta|/\tau}$$

$$\rho_W^{pPb} = \frac{W_{12}^{p+Pb}}{W_{12}^{pp}}$$

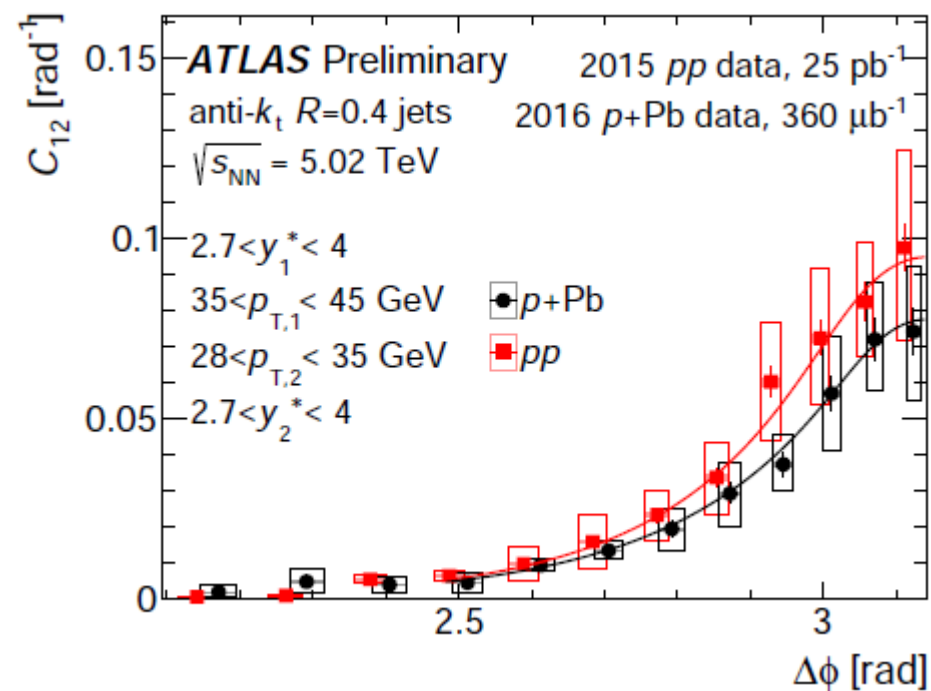
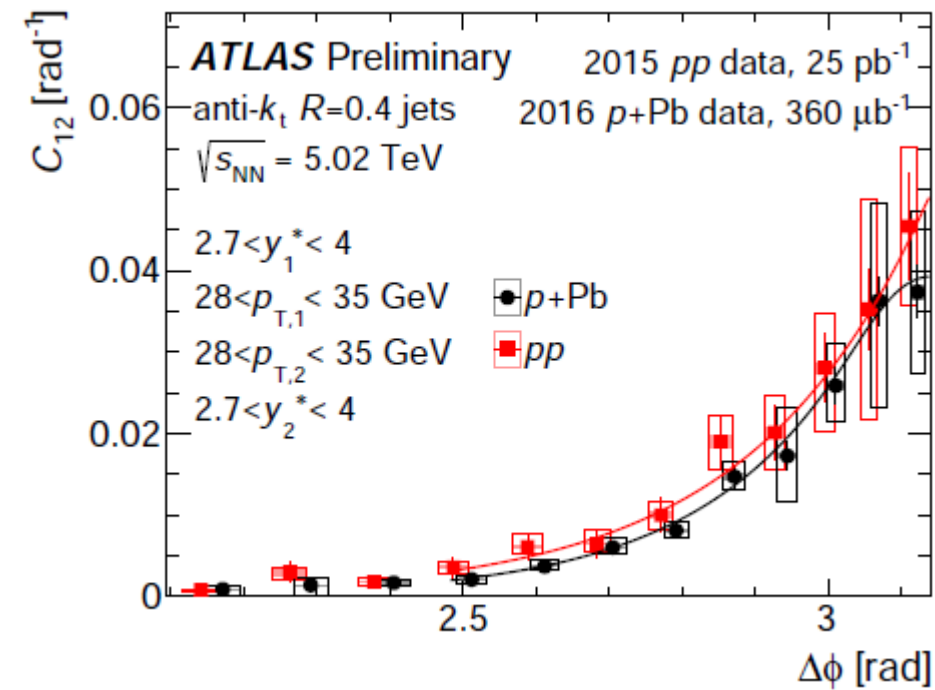
$$\rho_I^{pPb} = \frac{I_{12}^{p+Pb}}{I_{12}^{pp}}$$

W_{12} fitted to reduce
impact of
statistical fluctuations



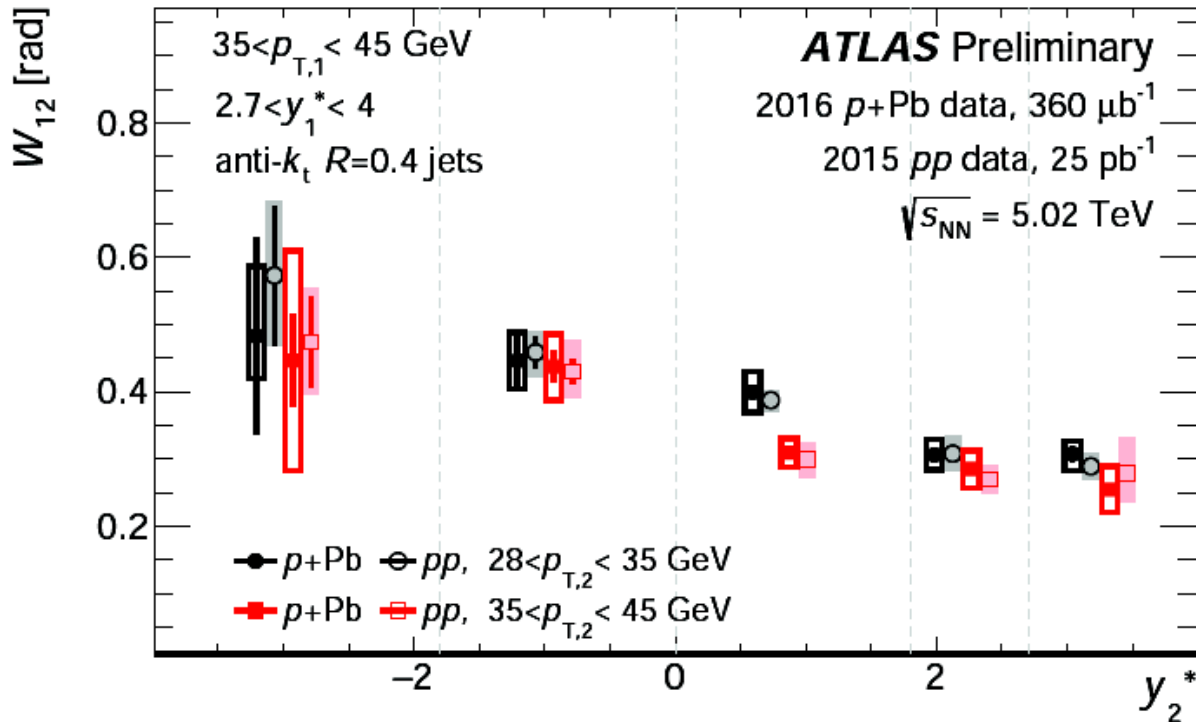
- Measurement performed in $-4.0 < y^* < 4.0$ and for $28 < p_T < 90$ GeV.
- Good jet reconstruction performance even in the forward region.
- Residual departure of JES from unity corrected by unfolding.

C_{12} distributions



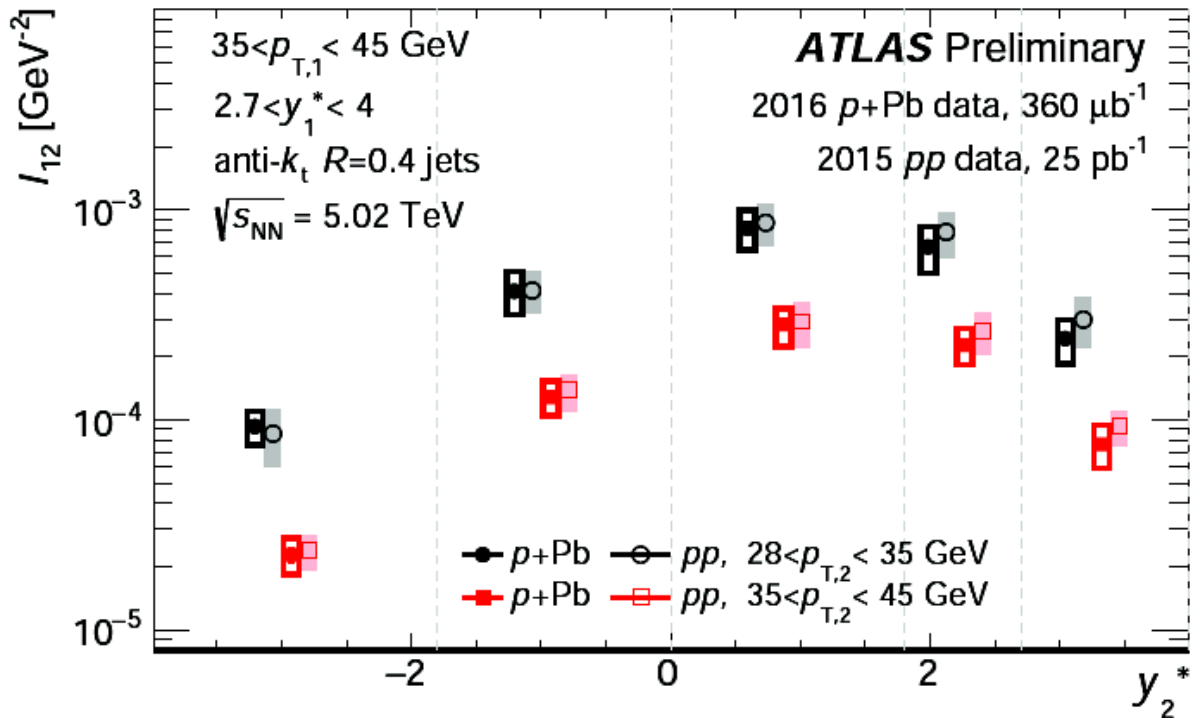
Lowest forward bin: kinematic selection corresponds to $1.5 \cdot 10^{-4} < x < 10^{-3}$

W_{12} distributions



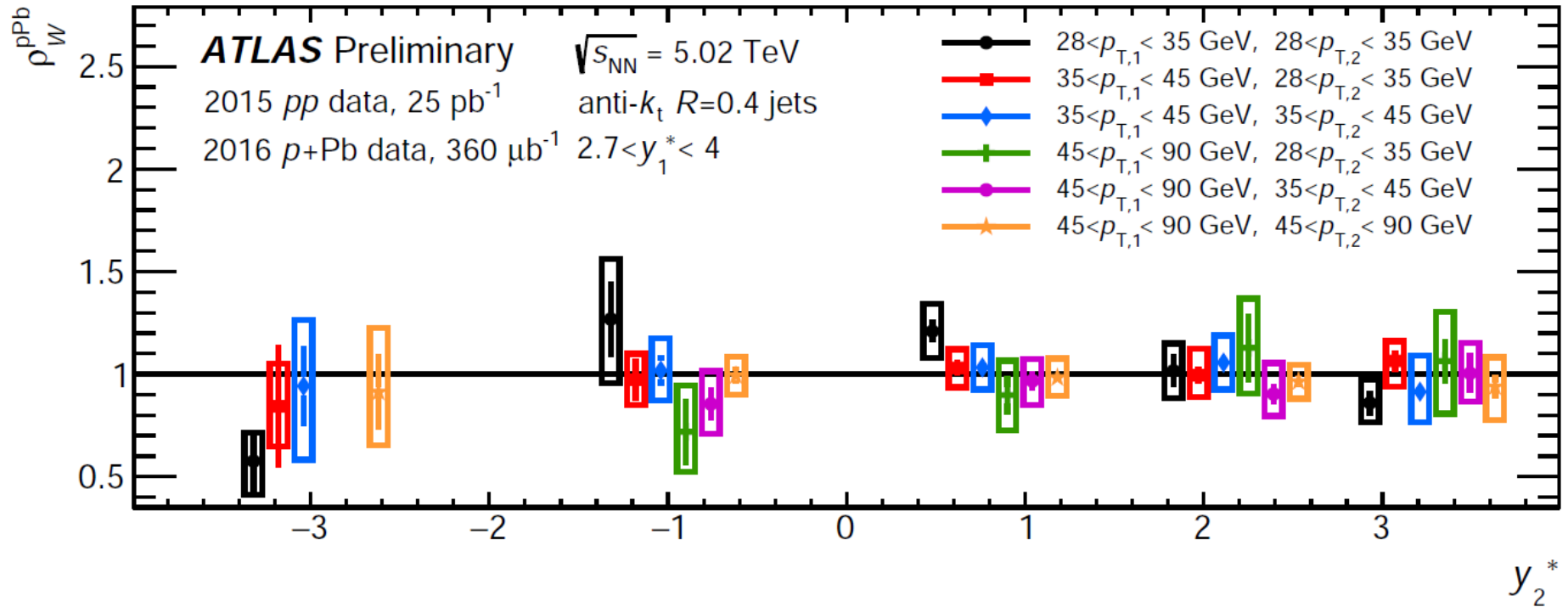
- Widths of azimuthal correlations **increase with increasing rapidity separation** between jets.
- Widths of azimuthal correlations **increase with increasing p_T imbalance** between jets.

I_{12} distributions



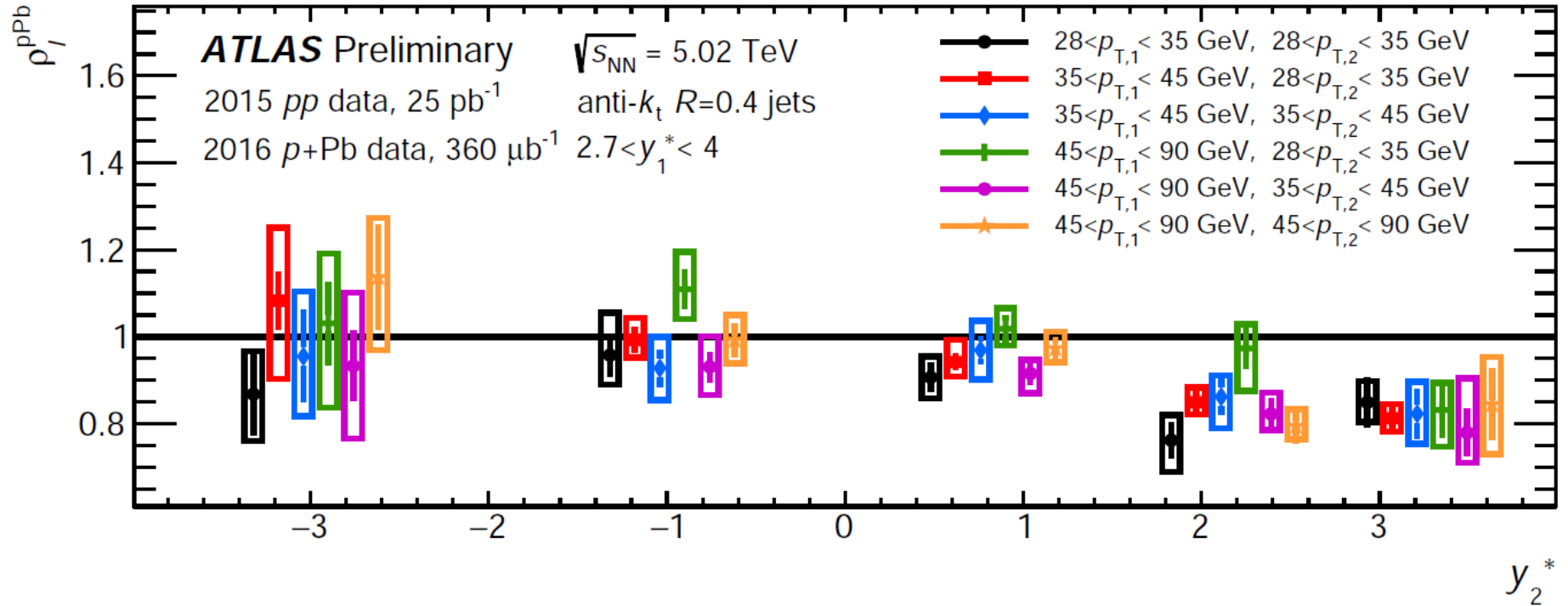
- Yields of jets: shape dictated by **faster fall-off of forward cross-section** as compared to inclusive cross-section.
- Measurement repeated also for a configuration with $\Delta p_T = p_{T,1} - p_{T,2} > 3 \text{ GeV}$ with the same conclusions.

ρ_W distributions



- No significant broadening of azimuthal correlations seen in $p+\text{Pb}$ compared to pp .

ρ_1 distributions



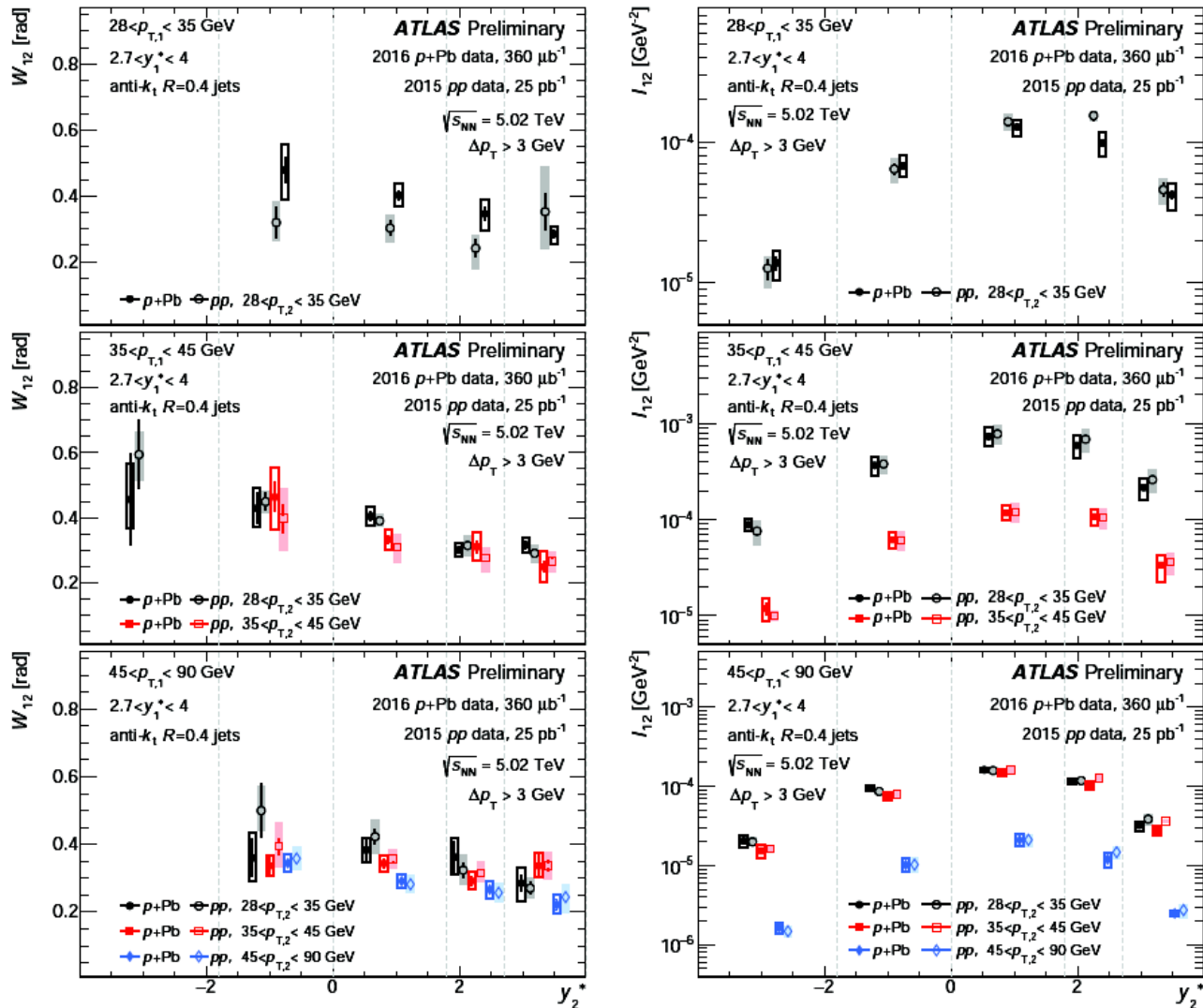
- **20% suppression** in yield seen for **forward-forward** jets in $p+\text{Pb}$ collisions in proton-going direction.

- Photons in p +Pb collisions at 8 TeV
 - Expected isospin effects seen.
 - No ability to distinguish nPDF effects.
 - No initial state energy loss observed in the data.
 - More p +Pb data needed to access nPDF effects with photons / electro-weak probes.
- Dijet $\Delta\phi$ correlations
 - No significant broadening of azimuthal correlations seen in p +Pb compared to pp .
 - 20% suppression in yield seen for forward-forward jets in p +Pb collisions compared to pp .
 - Should provide new input for saturation models.

Backup slides

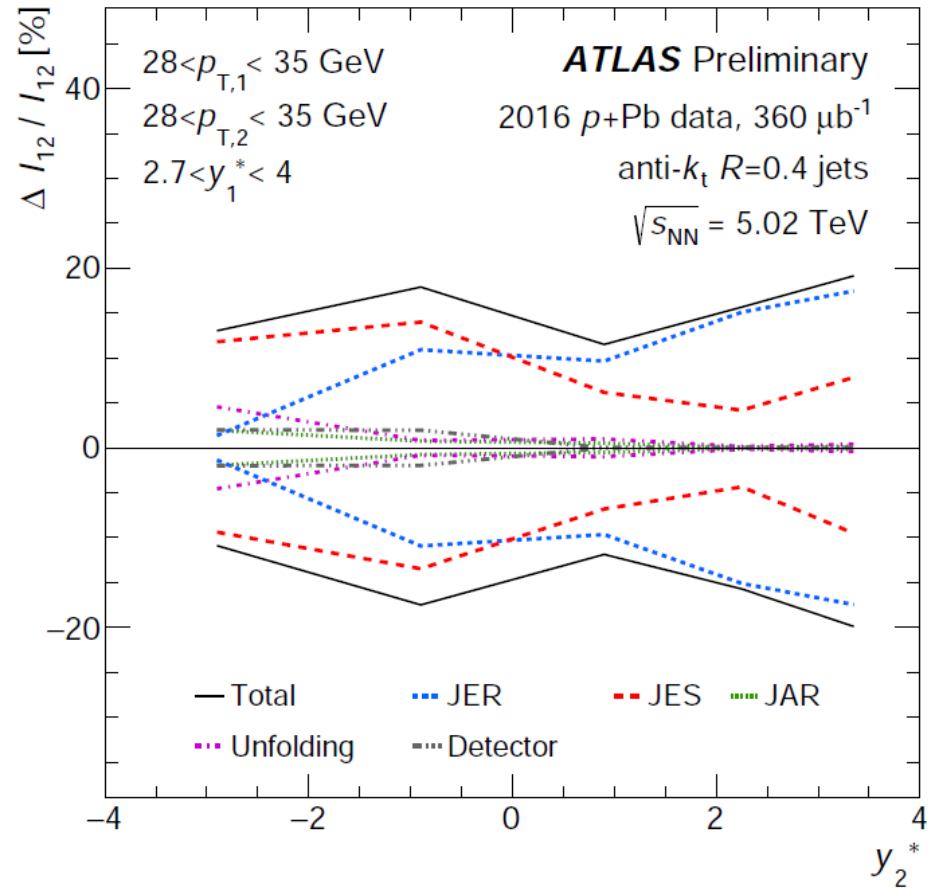
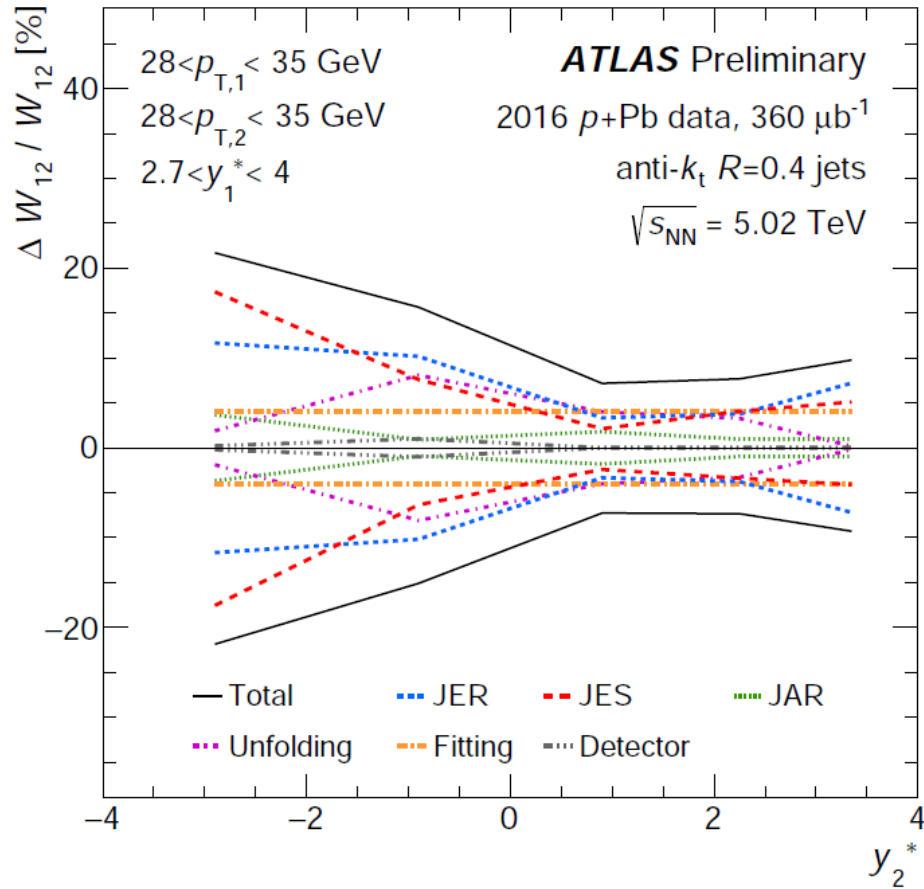


Full set of distributions



- Selection and purity of photons (10% at low E_T)
- Photon energy scale and resolution (5-10% at large E_T and η)
- Extrapolation (<5%)
- Reference pp spectra for R_{pPb} (< 12%)
- Luminosity (6.2%)
- Other small sources of uncertainties:
 - Generator level vs detector level isolation (<2%)
 - Data-taking period (1%)
 - Direct / fragmentation photon ratio in MC (1%)
 - Contribution of mis-reconstructed electrons from W, Z (<1%)

Systematic uncertainties



Fitting function



$$C_{12}(\Delta\Phi) = \int_{-\infty}^{\infty} d\delta \frac{e^{-\delta^2/2\sigma^2}}{\sqrt{8\pi\sigma^2\tau^2}} e^{-|\Delta\Phi-\delta|/\tau}$$

$$C_{12}(\Delta\Phi) = A \frac{e^{\sigma^2/2\tau^2}}{2\tau} \left(\frac{1}{2} e^{\Delta\Phi/\tau} \operatorname{Erfc} \left(\frac{1}{\sqrt{2}} \left[\frac{\Delta\Phi}{\sigma} + \frac{\sigma}{\tau} \right] \right) + e^{-\Delta\Phi/\tau} \left[1 - \frac{1}{2} \operatorname{Erfc} \left(\frac{1}{\sqrt{2}} \left[\frac{\Delta\Phi}{\sigma} - \frac{\sigma}{\tau} \right] \right) \right] \right)$$

Bins in $p_{T,1}$ [GeV]	Bins in $p_{T,2}$ [GeV]	Bins in y_2^*
$28 < p_{T,1} < 35$	$28 < p_{T,2} < 35$	$2.7 < y_2^* < 4.0$
$35 < p_{T,1} < 45$	$35 < p_{T,2} < 45$	$1.8 < y_2^* < 2.7$
$45 < p_{T,1} < 90$	$45 < p_{T,2} < 90$	$0.0 < y_2^* < 1.8$
		$-1.8 < y_2^* < 0.0$
		$-4.0 < y_2^* < -1.8$